Unexpected Trends in Copper Removal from Aβ Peptide: When Less Ligand Is Better and Zn Helps

Charlène Esmieu, Raúl Balderrama-Martínez-Sotomayor, Amandine Conte-Daban, Olga Iranzo, Christelle Hureau

Unexpected trends in Copper removal from Aβ peptide: when less ligand is better and Zn helps.

Charlène Esmieu (a), Raúl Balderrama-Martínez-Sotomayor (b), Amandine Conte-Daban (a), Olga Iranzo (b)* and Christelle Hureau (a)*

(a) CNRS, LCC (Laboratoire de Chimie de Coordination) 205 route de Narbonne, BP 44099 31077 Toulouse Cedex 4, France

(b) Aix Marseille University, CNRS, Centrale Marseille, iSm2, Campus Scientifique de St Jérôme, 13397 Marseille Cedex 20, France

Keywords: bioinorganic chemistry / ligands / speciation / Alzheimer's disease / ROS / Copper

Abstract

Cu, Zn and amyloid-β (Aβ) peptides play an important role in the etiology of Alzheimer's disease (AD). Their interaction indeed modify the self-assembly propensity of the peptide that is at the origin of the deposition of insoluble peptide aggregates in the amyloid plaque, a hallmark found in AD brains. Another even more important fallout of the Cu binding to Aβ is the formation of Reactive Oxygen Species (ROS) that contributes to the overall oxidative stress detected in the disease and is due to the redox ability of the Cu ions. Many therapeutic approaches are currently developed to aid fighting against AD, one of them targeting the redox active Cu ions. Along this research line, we report in the present article the use of a phenanthroline-based peptide like ligand (L) which is able to withdraw Cu from Aβ and redox silence it in a very stable 4N Cu(II) binding site even in the presence of Zn(II). In addition and in contrast to what is usually observed, the presence of excess of L do lessen the searched effect of ROS production prevention but it is counterbalanced by the co-presence of Zn(II). To explain such unprecedented trends we proposed a mechanism that involves the redox reaction between Cu(II)L and Cu(I)L_2. We thus illustrated (i) how speciation and redox chemistry can weaken the effect of a ligand that would have appeared perfectly suitable if only tested in 1:1 ratio and on CuAβ and (ii)

how Zn overcomes the undesired lessening of ROS arrest due to excess of ligand. In brief, we have shown how working in biological relevant conditions is important for the understanding of all the reactions at play and this must be taken into consideration for the further rational design of ligands aiming to become drug-candidates.

Introduction

Alzheimer disease (AD) is the most common neurodegenerative disease in the elderly,[1] notably characterized by β-amyloids peptide (Aβ) deposits in the brain constituting the senile plaques.[2] The causes of AD are still not clearly identified but several evidences highlight the involvement of metal ions in the pathogenesis of the disease. More specifically, it has been shown over decades of intensive research that Aβ peptide possesses the ability to bind metal ions,[3, 4] and that senile plaques are enriched in copper, zinc and iron (Cu, Zn and Fe).[5, 6] When bound to Aβ peptide, it has been shown that Cu do keep the propensity to produce reactive oxygen species (ROS) due to its redox ability, although to a lesser extent. The toxicity associated to the CuAβ-induced ROS is more linked to the places where the ROS are produced rather than to the level of ROS produce.[7] These ROS contribute to the overall increase of the oxidative stress linked to the development of the disease.[3] The ROS production is catalyzed by an intermediate species called the "in between state" (IBS) where it has been proposed that the Cu is bound to Aβ peptide by the N-terminal amine, the carboxylate group from Asp1, and one imidazole group from one His ring of the peptide. In this particular geometry the Cu can cycle between its two redox states +I and +II.[8, 9] In the brain, ascorbate, a biological reductant, and O_2 can fuel the reaction by respectively reducing and oxidizing the Cu in the IBS leading to the formation of ROS. The properties of the Aβ peptides to bind Cu(II/I) and Zn(II) have also been intensively studied in the last decade.[3, 4, 10, 11] Cu(II) is mainly bound by the N-terminal amine, the carbonyl function from Asp1-Ala2 peptide backbond and two imidazole rings from His6/His13/His14 with a conditional affinity of 10^{10} M^{-1} at pH 7.4.[12-14] Cu(I) coordination has been less investigated, most probably Cu(I) lies in a dyad of His rings[15, 16] with proposed affinities values ranging from 10^7 M^{-1} to 10^{10} M^{-1} with no consensus reached.[15, 17-20] Zn(II) coordination site is mainly made by two His residues and two carboxylates, with the predominant contribution of Glu11, with an affinity ranging from 10^5 M^{-1} to $10^6 M^{-1}$.[4, 12] Aβ possesses thus a high Cu(II) over Zn(II) selectivity which is about 2 to 3 orders of magnitude at neutral pH.

To alter CuAβ toxicity, which is recognized as a key event in the AD development, Cu chelators have been developed. A large range of chemical families has been investigated to remove Cu (mainly Cu(II))

from Aβ including multi-targeting drugs.[21-23] It has been shown that several parameters are important for the ligand to be adapted in the AD context.[21] Investigations of diverse families of Cu chelators led to the determination of what can be called "prerequisites". The essential parameters to be considered for ligand design/selection should include (1) Cu affinity (higher than Aβ) and (2) selectivity (over Zn(II) since this metal ion is present in the synaptic cleft and in the senile plaques at higher concentrations than Cu, *i.e*. 1-10 µM for Cu and 10-300 µM for Zn(II) under neuronal excitation[24, 25] in the synaptic cleft and 0.4 mM for Cu and 1 mM for Zn(II) in the senile plaques)[3, 5, 26], (3) the redox silencing of the Cu (Cu(I) and Cu(II)),[27] (4) the kinetics factors of Cu removal,[28] (5) the ability to cross the brain-blood-barrier (BBB), (6) the metabolic stability and (7) the intrinsic harmlessness.[21]

Nevertheless, the speciation of Cu in its two redox states with respect to its ROS production ability has never been investigated so far. This is the purpose of the present study where the ligand L (Figure S1) has been selected to illustrate such effect based on (i) the possibility of forming 1:1 complex and the well-known 2:1 species, (ii) the formation of two different binding sites for Cu(I) and Cu(II) while fulfilling most of the redox, thermodynamic, kinetic criteria described above. In addition, the ligand can be further implement with peptides aiding to enter the BBB.[29]

Herein we report the study of a phenanthroline-based peptide like ligand (L, Figure S1) with a well-defined Cu(II) coordination cavity. L coordinates Cu(II) giving rise to a single major species where Cu(II) displays a distorted squared planar geometry (Figure 1).[30] This complex is stable in a wide range of pH (from 3.0 to 9.0) and its conditional affinity ($K_{Cu(II)L,\ cond}$) at pH 7.1 is $1.99x10^{14}$ M^{-1} (Cu(II)L). Cyclic voltammetry studies at that pH revealed a non-reversible redox process Cu(II) ⇄ Cu(I).[31] Namely, L shows a cathodic (E_{pc} = − 0.452 V) and an anodic peak (E_{pa} = 0.201 V) with a peak to peak separation $\Delta E_p = E_{pa} - E_{pc}$ = 0.653 V (V *vs* Ag/AgCl). Taking into account these properties, *i.e*. high affinity constants for Cu(II), a non-reversible Cu(II) ⇄ Cu(I) redox process, and the fact that L can be easily functionalized for further targeting (multi-targeted purpose), L was explored in the context of AD.

The ligand L is capable of arresting Cu and CuAβ-induced ROS production at 1:1 ligand:Cu ratio even in presence of Zn(II). This is due to capture or removal from Aβ of Cu(II) to form the Cu(II)L complex resistant to reduction. This property is lessened when L is present in excess but can be recovered in the concomitant presence of Zn(II). These intriguing features are under focus in this study and are attributed to an alternative redox cycling mechanism implying Cu(I/II)L_2 as the active species in ROS production. These results highlight the complexity of the multifactorial ROS production process and the importance of carrying out the experiments under conditions closer to the biological relevant ones.

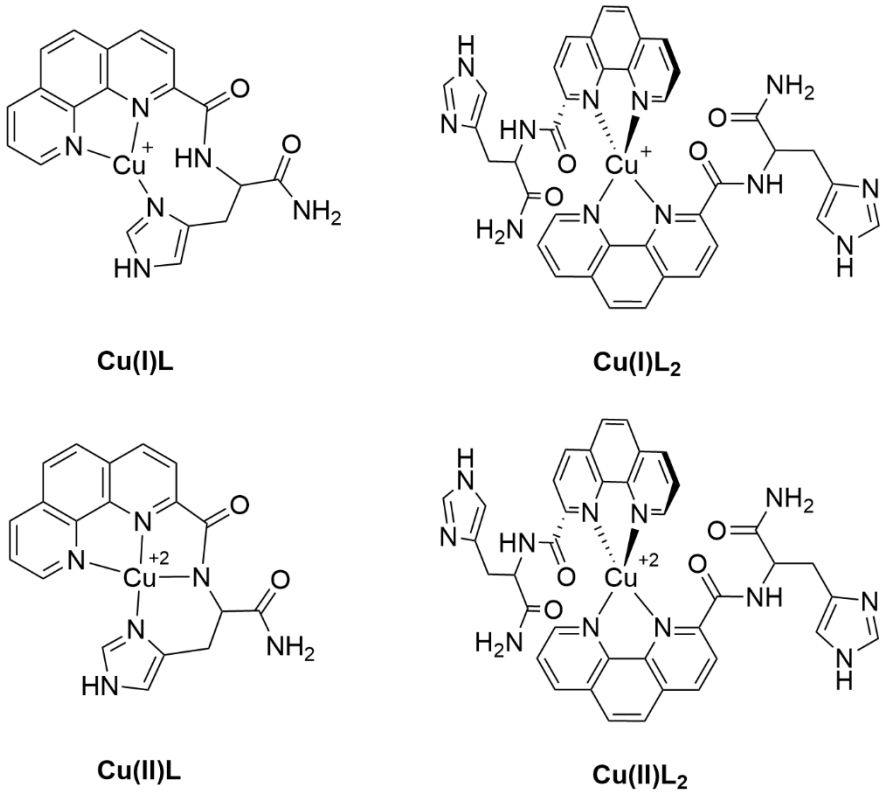

Figure 1. Chemical structures proposed for the species Cu(I)L, Cu(I)L_2, Cu(II)L and Cu(II)L_2

Results and discussion

Preliminary ROS experiments

The potential of L (Figure S1) and of its carboxylic derivative L' (Figure S1) to arrest ROS production was analyzed by monitoring ascorbate ($AscH^-$) consumption at 265 nm using UV-vis spectroscopy.[32] These ligands were evaluated in two different ways (Figure S1A and B). (i) Starting from the mixture of

Cu(II)/Cu(I): in this assay the correspondent ligand is added after the ascorbate consumption has started by the addition of Cu(II). (ii) Starting from Cu(I): in this experiment Cu(II) is initially reduced to Cu(I) by ascorbate under anaerobic conditions and then the corresponding ligand is added. Subsequently, air (O_2) is introduced to the system. The results obtained reflect the different capability of L and its carboxylic derivative L' to arrest ascorbate consumption, *i. e.* ROS production. Clearly, L slows down significantly the ascorbate consumption in both experiments, while its carboxylic derivative can only mildly decrease it. These data are in agreement with previous published studies where it was observed that the Cu complex of the carboxylic derivative generated more ROS species and thus, it was a better DNA cleaving agent.[30] L was selected for further studies in the context of AD.

Spectroscopic and thermodynamic parameters of L complexes

For the sake of simplicity the protonation state of the ligand in the complexes will not be described. Therefore, for the case of Cu(II) the complex Cu(II)LH_{-1} (deprotonation of the amide) will be denoted as Cu(II)L.

The Cu(II) apparent binding constant of L at pH 7.1 ($K_{Cu(II)L,\ app}$ = 3.55x10^{12} M^{-1}, Table 1) was directly calculated from the conditional binding constant value ($K_{Cu(II)L,\ cond}$ = 1.99x10^{14} M^{-1}) obtained by potentiometric studies using the Equation 1 described in experimental section.[33] This model considers the buffer contribution at a given pH and concentration.

The binding of Cu(I) to L was monitored by UV-vis spectroscopy under anaerobic conditions. Namely, the UV-vis spectra were recorded upon successive additions of an acetonitrile (ACN) solution of the tetrakis(ACN)Cu(I) hexafluorophosphate salt (from 0 to 3.0 equiv. of Cu(I)) to a solution of 200 µM L in 100 mM HEPES buffer (Figure S2). The spectra were analyzed and fit using HypSpec (HYPERQUAD suit of programs).[34] The values for the apparent binding constants are reported in Table 1 (see Table S1 for equilibria definition) and the speciation diagram under the current experimental conditions is reported in Figure S2. These data indicate that L can form the complexes Cu(I)L and Cu(I)L_2 as reported for phenanthroline ligand.[35-37] The binding affinity of the first unit of L to Cu(I) (Cu(I)L) is higher than that

of the phenanthroline ligand due to the presence of an extra coordination site, *i.e.* the His residue. On the other hand, the binding of the second unit of L ($Cu(I)L_2$) is weaker most likely due to the steric hindrances introduced by this His. The proposed structures for the complexes Cu(I)L and $Cu(I)L_2$ are presented in Figure 1.

The Zn(II) apparent binding constant ($K_{Zn(II)L,\ app}$) was determined at pH 7.1 by UV-vis spectroscopy. UV-vis spectra were recorded upon successive additions of $Zn(NO_3)_2$ (from 0 to 2 equiv. of Zn(II)) to a solution of 50 µM L in 100 mM HEPES buffer (Figure S3). The $K_{Zn(II)L,\ app}$ is reported in Table 1.

Table 1. Apparent affinity constants (K_{app}) of Cu(II), Cu(I) and Zn(II) binding to L and Aβ in HEPES buffer (100 mM, unless otherwise noted) at pH 7.1.

	K_{app} (M^{-1})	log K_{app}	Entries
Cu(II)L [(a)]	3.5×10^{12}	12.5	1
Cu(I)L	6.3×10^{6}	6.5	2
$Cu(I)L_2$	6.3×10^{10}	11.3	3
Zn(II)L	7.6×10^{5}	5.9	4
Cu(II)Aβ [(b)]	2.8×10^{7}	7.5	5
Cu(I)Aβ [(c)]	7.5×10^{6}	6.9	6
Zn(II)Aβ [(d)]	1.1×10^{5}	5.0	7
Selectivity of L[(e)] : $\sigma = 4.6 \times 10^{6}$ **Selectivity of Aβ[(e)] :** $\sigma = 2.5 \times 10^{2}$			8

(a) Calculated from the $K_{Cu(II)L,\ cond}$ (1.99×10^{14} M^{-1}) obtained by potentiometric studies.[30]
(b) Calculated from the $K_{Cu(II)A\beta,\ cond}$ (1.6×10^{9} M^{-1}) reported in reference [14]
(c) Value determined at pH 7.4.[18] This means that the value here is an overestimation of the value at pH 7.1 and cannot be directly compared with the other values.
(d) Value obtained in 50 mM HEPES.[38]
(e) $\sigma = \frac{K^{L}_{Cu}}{K^{L}_{Zn}}$, calculated for Cu(II) *vs* Zn(II)

While the data reported in Table 1 indicate that L is thermodynamically capable to fully remove Cu(II) from Aβ peptide (entry 1 *vs* 5 in Table 1) even in the presence of Zn(II) (entry 8 in Table 1), they show that the reaction between L and Aβ for Cu(I) binding is equilibrated (entry 2 *vs* 6 in Table 1).

The EPR spectrum (Figure S4A) of a solution containing L and 0.9 equiv. of $Cu(NO_3)_2$ (190 µM) in 100 mM HEPES buffer pH 7.1 is consistent with the EPR data reported previously for the Cu(II)L complex[30] and corroborates its formation under the current experimental conditions. The addition of an excess

of L (10 equiv. *vs* Cu(II)) does not modify the EPR signature (Figure S4) indicating that the Cu(II)L_2 species does not form under the current experimental conditions. The UV-vis spectrum of Cu(II)L displays a characteristic d-d absorbance at 605 nm while Cu(I)L has a transition at 420 nm attributed to metal-to-ligand charge transfer in accordance with previous reports (Figure S4B and Table S2).[39, 40] Consistent with EPR data, the formation of a Cu(II)L_2 is not observed by UV-vis in excess of L (10 equiv., Figure S4B). Conversely, addition of another equiv. of L to Cu(I)L leads to a spectrum modification with an increase of the absorbance at 420 nm mirroring the formation of the Cu(I)L_2 complex (Figure S4B). However, the co-existence of the two Cu(I)L and Cu(I)L_2 species precludes a complete assignment of the spectra.

*Spectroscopic monitoring of Cu(II) and Cu(I) removal from A*β

Different spectroscopic techniques have been applied in order to confirm the ability of L to retrieve Cu(II) from CuAβ, both in the absence and presence of Zn(II). Indeed, the UV-Vis, XANES and the EPR signatures are easily distinguishable between Cu(II)Aβ and Cu(II)L.

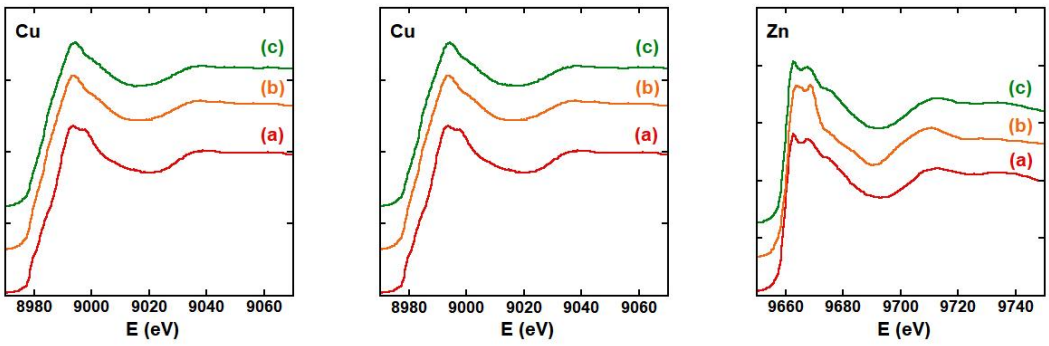

Figure 2. Left panel: XANES at Cu edge of (a) CuAβ ; (b) CuL and (c) CuAβ + L. Middle and right panel: XANES at Cu(II) and Zn(II) edge of (a) MAβ (M = Cu or Zn); (b) ML (M = Cu(II) or Zn(II)) and (c) Cu ,Zn-Aβ + L. [peptide] = [L] = [Cu] =[LZn] = 1 mM; HEPES buffer 100 mM pH 7.1. 10 % glycerol are used as a cryoprotectant. T = 20 K. On the y-axis, every interval correspond to 0.5 intensity unit of normalized spectra.

The XANES (X-ray Near Edge Absorption Structure) is a very-well suited method to monitor the exchange of Cu between the Aβ peptide and the L ligand, even in presence of Zn(II). Indeed those two metals can be monitored during the same experiment due to the proximity in the edge of Cu(II) and Zn(II). We thus monitor the removal of Cu(II) from the Aβ peptide by L in the absence and presence of Zn(II). The superimposable fingerprints of Cu(II)L, Cu(II)Aβ + L and their difference with Cu(II)Aβ (left panel in Figure 2), indicate that Cu(II) is fully removed from the Aβ peptide by the ligand in full agreement with the affinity parameters (Table 1). Similarly, the superimposable fingerprints of Cu(II)L and Cu(II)Aβ + Zn(II)L for the Cu edge (middle panel in Figure 2) and of Zn(II)Aβ and Cu(II)Aβ + Zn(II)L for the Zn(II) edge (right panel in Figure 2) indicate that a complete metal swap between the two complexes occurs, in line with the selectivity parameters (Table 1).

A similar competition followed by EPR confirms that in presence of 1.2 equiv. of L the Cu(II) is totally removed from Cu(II)Aβ even in presence of 1.2 equiv. or 10 equiv. of Zn(II). Indeed, the EPR spectrum of a mixture of L, Aβ, Cu(II) and Zn(II) is identical to the one of Cu(II)L (Figure S4B). Same results have been obtained with UV-vis spectroscopy. A mixture of Cu(II)Aβ + L lead to a spectrum featuring the d-d transition corresponding to the Cu(II)L species (Figure S5A).

In brief, in agreement with the thermodynamic parameters (Table 1), L is able to extract Cu(II) from Aβ regardless the presence of Zn(II) (up to 10 equiv.).

Additionally, the competition experiment has been performed in presence of Cu(I), in a sealed UV-vis cuvette under argon (Figure S5B). Compared to the spectrum in absence of Aβ, the feature at 420 nm characteristic of Cu(I)L and Cu(I)L_2 species is less intense (by about 25%) indicating a contribution in the spectrum of Cu(I)Aβ that doesn't absorb in this domain. This trend is in line with the respective apparent binding constants of Cu(I)Aβ and Cu(I)L (Table 1).

ROS experiments under biological relevant conditions

The ability of L to prevent and stop the CuAβ-induced ROS formation was investigated in a buffered medium at pH 7.1 with an ascorbate consumption assay (for more detail see the experimental part).[27,

[32, 41] The studies were conducted in absence and in presence of Zn(II) ions to mimic the synaptic cleft environment, a place where Zn(II) ions are also present and in higher concentration than Cu ions.[41]

We first studied the ability of Cu(II)L to generate ROS by its own in presence of an excess of reductant (Figure S6A). Ascorbate is not consumed in presence of Cu(II) and L, illustrating the formation of Cu(II)L which is resistant to the reduction by ascorbate, in accordance with its reduction potential determined previously.[30] In presence of Cu(II)Aβ and 1.2 equiv. of L, again the ascorbate is not consumed (Figure S6B). L is thus able to prevent the ascorbate consumption in presence of Cu(II)Aβ, in line with its ability to withdraw Cu(II) from Cu(II)Aβ and its resistance to ascorbate reduction. The ability of L to prevent the ROS production is not decreased in presence of 1.2 equiv. of Zn(II) in line with the appropriate selectivity for Cu(II) over Zn(II) (Figure S6C and Table 1).

L is also able to prevent the ROS production starting from the reduced Cu(I) and Cu(I)Aβ as proven by the absence of ascorbate consumption (Figure S7A and B). However, L does not form an air-stable Cu(I) complex and upon exposure to air (O_2), the quick appearance of a d-d transition band characteristic of the formation of the Cu(II)L complex in UV-vis spectroscopy demonstrates that the final product precluding the formation of ROS is the redox stable Cu(II)L (Figure S8). Addition of 1.2 equiv. of Zn(II) doesn't affect the prevention of ROS production (Figure S7C).

L has been further challenged to stop the CuAβ-induced ROS production under operating conditions, meaning that L has been added to a solution actively producing ROS through the reduction and the oxidation of CuAβ by ascorbate and O_2, respectively. This study, in conditions which are probably closer to the biological environment, shows the ability of L to stop the ROS production in presence of a mixture of Cu(II)/Cu(I) in the solution (Figure 3). Again, the presence of 1.2 equiv. of Zn(II) did not change the ligand's ability to prevent the formation of ROS (Figure 3B and D). Even more, the presence of Zn(II) ameliorates the performances of L by a 1.5 factor (Figure 3A, 1.2 L *vs* Figure 3B 1.2 L) (rates of ascorbate consumption of 4.3 ± 0.1 $nM.s^{-1}$ in presence of Zn(II) *vs* 6.5 ± 0.4 $nM.s^{-1}$ without Zn(II)).

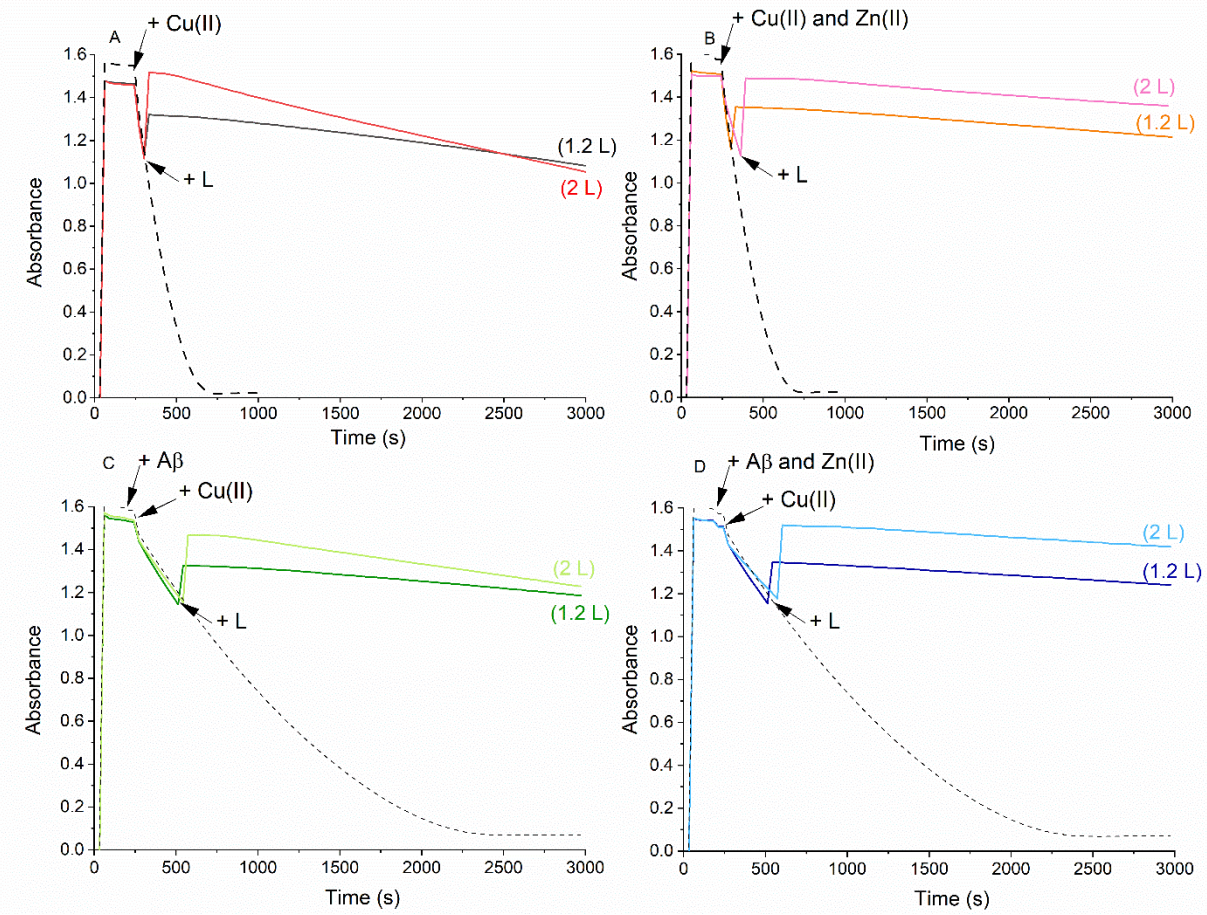

Figure 3. Kinetics of ascorbate consumption starting from a mixture of Cu(II)/Cu(I) in absence (panel A and B) or in presence of Aβ peptide (panel C and D) with one or two equivalents of L, without Zn(II) (panel A and C) or with Zn(II) (panel B and D), followed by UV-vis spectroscopy at 265 nm with a background correction at 800 nm. Panel A: Cu + L; Panel B : Cu + Zn(II) + L; panel C : CuAβ + L; panel D : CuAβ + Zn(II) + L. [Aβ] = [Zn] = 12 µM, [L] = 12 or 20 µM, [Cu^{2+}] = 10 µM, [$AscH^-$] = 100 µM, [HEPES] = 100 mM, pH 7.1. On the figure (1.2 L) and (2 L) mean that 1.2 equiv. or 2 equiv. of L were added respectively *vs* Cu. In all the panel, the dashed line are the control experiments meaning that every component has been added into the UV-vis cuvette except L. The arrows indicate the addition of each element.

The Cu(I) to L binding constant determination experiments indicate that L is able to form both 1:1 and 2:1 complexes with Cu(I) (Cu(I)L and Cu(I)L_2). The speciation of metal complexes in the biological medium is a key parameter as the ability of a ligand to reach its objective (here withdrawing Cu from

CuAβ) can be impacted by a change in the speciation of complex. For these two reasons, the ROS experiments were also undertaken in presence of two equiv. of L. It has to be noted that this type of analysis (excess of ligand) is barely reported in literature, especially with respect to Cu(I) as mentioned in the introduction. The same ROS experiments than those previously described with Cu(II), Cu(I) and a mixture of Cu(II)/Cu(I) with Aβ and 1.2 equiv. of L, were performed with 2 equiv. of L, in absence or in presence of Zn.

The experiment starting from a mixture of Cu(II)/Cu(I) led to a clear loss of efficiency when L is introduced in excess (2.0 equiv. of L *vs* Cu, Figure 3A, 2 L). With 2.0 equiv. of L the ROS production is slowed down, but not completely stopped as seen in Figure 3A for 1.2 L. This trend was confirmed by the stepwise addition of L from 1.0 to 2.0 by 0.2 equivalent increment (Figure S9A) that shows that the higher the excess of ligand, the higher the ascorbate consumption. Quantitatively, the rates of the consumption of ascorbate between 1500s and 3000s of the experiment are 10.6 ± 0.1 $nM.s^{-1}$ and 6.5 ± 0.4 $nM.s^{-1}$ for 2.0 equiv. and 1.2 equiv. of L, respectively (Figure 3A).

The experiment has been repeated with the Aβ peptide in solution (Figure 3C) and shows the same results; the excess of L enhances the ascorbate consumption (7.4 ± 0.1 $nM.s^{-1}$ and 3.2 ± 0.1 $nM.s^{-1}$ for 2.0 equiv. and 1.2 equiv. of L, respectively, Figure 3A).

In presence of Zn(II) (Figure 3B and D) the excess of L doesn't have any impact on the consumption of ascorbate both in absence or presence of Aβ. It can be shown that Zn(II) counteracts the effect of excess of ligand even in the course of ascorbate consumption (Figure S9B), which may be in line with the respective affinity constants of Zn(II) and Cu(I)L for L (Table 1); this will be discussed later in the text. Indeed after addition of Zn, the slope in presence of 2 equiv. of L reaches 4.1 ± 0.2 $nM.s^{-1}$, the weakest values observed when starting from a Cu(I)/Cu(II) mixtures.

To gain insight about the role of each redox state in this behavior, ascorbate consumption experiments were repeated with an excess of L starting either from Cu(I) or Cu(II). In both cases, the ascorbate consumption profile with 2 equiv. of L resembles the one with 1.2 equiv. (Figures S6 and S7) (1.9 ± 0.2

$nM.s^{-1}$ *vs* 2.4 ± 0.2 $nM.s^{-1}$ for Cu(I) and 1.8 ± 0.2 $nM.s^{-1}$ *vs* 2.7 ± 0.1 $nM.s^{-1}$ for Cu(II) for 1.2 equiv. and 2 equiv. of L respectively). The ability of L to prevent the ROS formation is globally maintained with 2 equiv. of L. For the Cu(II) situation the result obtained is consistent with the potentiometric data[30] and the EPR experiment reported here that show the formation of the redox inert Cu(II)L complex regardless of the excess of ligand. For the Cu(I) case, the formation of the species $Cu(I)L_2$ is possible (Table 1) and favored in presence of 2.0 equiv. of L (Table S3). However this has not a strong impact on the ROS production since the O_2 oxidation of $Cu(I)L_2$ is slower than that of Cu(I)L (Figure S8, Table S4) and hence the oxidation of Cu(I)L will drive the equilibrium to consume the $Cu(I)L_2$.

Proposed mechanism

In the course of the ROS experiments, we observe unusual results: (i) the addition of L in excess increases the ascorbate consumption and (ii) the presence of Zn(II) counteracts it. In addition, starting from either Cu(II) or Cu(I) leads to less ascorbate consumed versus starting from a mixture of the two redox-states.

To tentatively explain such observations, we propose the mechanism in Figure 4 (central part), as a working hypothesis. The final species of the whole mechanism is the Cu(II)L (green oval), the formation of which drives the other reactions. During ROS production, the Cu(II)L oxidizes the $Cu(I)L_2$ complex leading to Cu(I)L and $Cu(II)L_2$, respectively (equilibrium (a)), since $Cu(I)L_2$ is present even in slight excess of L (1.2 equiv., see Table S3). The $Cu(II)L_2$ formed can evolve along two paths either the decoordination of one L leading to the Cu(II)L resistant to ascorbate reduction (path (b)) or its reduction by ascorbate to $Cu(I)L_2$ (path (c)), while the two paths are in competition. We can anticipate that (i) going from $Cu(II)L_2$ to Cu(II)L implies a strong reorganization of the coordination sphere: from the $Cu(II)L_2$ species, one ligand has to decoordinate while the imidazole group from the His and the amide-bond from the remaining has to coordinate; the deprotonation of the amide bond prior to its coordination being required (See Figure 1) and (ii) the $Cu(II)L_2$ keeps the same geometry as in the $Cu(I)L_2$ (Figure 1) thus being easily reduced in line with redox potential values reported for related complexes.[35, 42-45] The

Cu(I)L formed can be oxidized to Cu(II)L (path (d)) or can bound an additional L ligand leading to $Cu(I)L_2$ in equilibrium with Cu(I)L (path (e), see Tables 1 and S1). The Cu(II)L + $Cu(II)L_2$ redox reaction is in line with the higher consumption of ascorbate detected when starting from a mixture of Cu(I)/Cu(II).

In the mechanism, the $Cu(I)L_2$ which is the only species that can mediate the reduction of Cu(II)L in our conditions, is favored in excess of L, while Cu(II)L cannot directly be reduced by ascorbate. This explains why ascorbate consumption is higher in presence of 2 equiv. of L that favors the formation of $Cu(I)L_2$ (compared to 1.2 equiv. of L, Table S3).

The effect seen in presence of Zn(II) agrees with the consumption of excess of ligand leading to a weaker stoichiometry of available L via the formation of the Zn(II)L species which is thermodynamically favored compared to the formation of $Cu(I)L_2$ from Cu(I)L (Table 1, Table S2). This will disadvantage the formation $Cu(I)L_2$ species and eventually lead to weaker ascorbate consumption.

In presence of Aβ (Figure 3C and 3D), L is able to lessen significantly the consumption of ascorbate, regardless of the conditions. The new reactions due to the presence of Aβ are (i) modification of the speciation between Cu(I), Cu(I)L and $Cu(I)L_2$ (equilibrium (f), and Table S4), (ii) of Cu(II) and Cu(II)L and (iii) the rapid formation of Cu(II)L *via* Cu(II)Aβ coming from oxidation of Cu(I)Aβ (reaction (g)). Based on the Cu(II) affinity (10^{12} *versus* 10^{7} for Aβ) and the Cu(II) over Zn selectivity of L (4.7×10^{6} *versus* 2.5×10^{2} for Aβ), it is expected that there is no change in Cu(II) speciation upon addition of Aβ (point (ii) above). With respect to points (i) and (iii), because the effects of ligand in excess and of Zn(II) are similar with or without Aβ, we anticipated that those Aβ-related new reactions either don't significantly contribute to the main redox reaction (Cu(II)L + $Cu(I)L_2$) or have counterbalanced effects. Having a more quantitative kinetic analysis is beyond the scope of the present study.

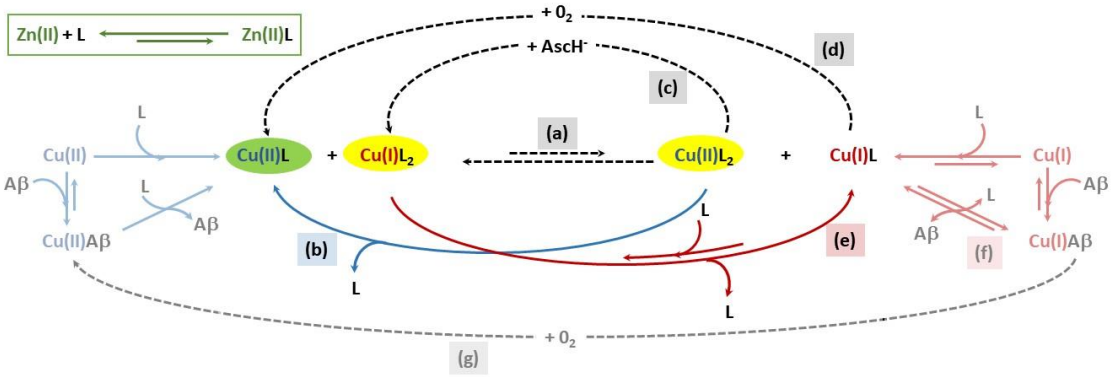

Figure 4. Proposed mechanism to explain the increased ascorbate consumption in presence of both Cu(I) and Cu(II) and super-stoichiometric ratio of ligand. Cu(II), Cu(I) and Zn(II) species are in blue, red and green, respectively. Yellow versus green ovals indicate ascorbate and O_2 consuming *versus* ascorbate resistant species. Plain and dashed lines correspond to speciation and redox reactions, respectively. Reaction implying the Aβ peptide are shadowed. For the sake of clarity, only processes key for the ROS production are shown and paths (a) to (f) are explained in the text.

Conclusion

Studies where the impact in ROS production of the Cu speciation in its different two oxidation redox states is investigated are barely carried out when exploring the chelation capabilities of designed ligands for chelation therapy in the AD context. For the first time, we have evidenced here that the use of ligands able to form 2:1 (L:Cu) species, independently of the redox state of the metal, can significantly increase the number of the reactions at play in the extraction of Cu ions from Aβ and their redox silencing. We have shown that super-stoichiometric ratio of L can be deleterious by lessening the ability of L to stop Cu(I/II) and Cu(I/II)Aβ induced ROS production. But if L has an appropriate affinity for Zn(II), then Zn(II) can counteract the undesired impact of the ligand in excess. This might be a biologically relevant process since there is a lot of Zn(II) in the synaptic cleft and we can anticipate that Zn(II) can buffer the available level of L.

We are currently working on a second generation of ligands that can either include tethering of BBB penetrating peptides or Aβ-targeting units. In such modified ligands, the sterical hindrance introduced by the functionalization may help precluding the formation of 2:1 species.

Experimental

All chemicals are from Sigma-Aldrich chemicals and TCI chemicals.

$A\beta_{16}$ (referred as Aβ) peptide (DAEFRHDSGYEVHHQK) was bought from Genecust. L and L' were synthesized following a published protocol.[30]

Stock solutions

All the stock solutions were prepared in milliQ water (resistance: 18.2 MΩ.cm).

HEPES buffer (sodium salt of 2-[4-(2-hydroxyethyl)piperazin-1-yl]ethanesulfonic acid) was prepared at an initial concentration of 500 mM, pH 7.1.

Cu(II) stock solutions were prepared from $CuSO_4.5H_2O$ salt at 100 mM or from $CuCl_2$ salt and standardized by titration with K_2H_2EDTA following standard methods,[46] and confirmed by ICP.

The stock solution of tetrakis(ACN)Cu(I) hexafluorophosphate (10.1 mM) was freshly prepared in ACN from the analytical grade Cu salt and stored under anaerobic conditions (*i.e.* inside a glovebox). The concentration was determined by UV-vis spectroscopy (ε_{483nm} = 13 300 M^{-1} cm^{-1}) using a 4-fold excess of bathocuproine in water as reported by Smith and Wilkins.[47]

Zn(II) stock solutions were prepared from a $ZnSO_4.7H_2O$ or from $Zn(NO_3)_2$ salts at 100 mM.

Sodium ascorbate was prepared at 5 mM and freshly used.

The L, L' and Aβ stock solutions were prepared at around 3 mM by dissolving the powder in milliQ water. Aβ was titrated by UV-vis using the Tyrosine chromophore, with $\varepsilon_{276\ nm}$ = 1410 $cm^{-1}M^{-1}$ at acidic pH. The precise concentration of L was determined by Cu(II) titration with a solution of known concentration using the d-d transition absorption of the complex to determine the equivalence point or by using the extinction coefficient of the phenanthroline at pH 7.4 in 100 mM TRIS-HCl buffer (ε_{268}

$_{nm}$ = 22 095 M^{-1} cm^{-1}). The concentration of L' was determined simply using the extinction coefficient of the phenanthroline. The L, L' and Aβ peptide stock solutions were stored at -20 °C.

UV/Visible spectrophotometry.

Apparent binding constants. The conditional affinity constant of L for Cu(II) (log $K_{Cu(II)L,cond}$ = 14.3 at pH 7.1) was obtained from potentiometric studies[30] using the following equation: K_{cond} = Σ conc. all complex species / [(Σ conc. ligand species not bound to Cu) x (Σ conc. Cu species not bound to ligand).[48]

Conditional binding constants were transformed in apparent binding constants in HEPES buffer using the Equation 1 [33], where L = L or Aβ, [HEPES] = molar concentration of used buffer, $\beta_{Cu(II)-HEPES}$ = $10^{3.22}$ and pK_{aHEPES} = 7.41.

$$\log K_{Cu(II)L,app} = \log K_{Cu(II)L,cond} - \log\left(1 + \beta_{Cu(II)-HEPES} + \frac{[HEPES]}{1+10^{-pH+pKa}}\right) \quad \text{Eq. 1}$$

The apparent affinity constant of L for Cu(I) ($K_{Cu(I)-L,app}$) was calculated in 100 mM HEPES buffer at pH 7.1 on a Varian Cary 60 Bio spectrophotometer. Spectra were recorded upon successive additions of Cu(I) (tetrakis(ACN)Cu(I) hexafluorophosphate) (from 0 and up to 4 equiv.) to a solution containing 200 µM of L under anaerobic conditions (inside a glove box). The spectra were analyzed and fit using HypSpec (HYPERQUAD suit of programs)[34]

The apparent affinity constant of L for Zn(II) ($K_{Zn(II)L,app}$) was calculated in 100 mM HEPES buffer at pH 7.1 on a Varian Cary 60 Bio spectrophotometer. UV-vis spectra were recorded upon successive additions of Zn(II) ($Zn(NO_3)_2$) (from 0 to 2 equiv. of $Zn(NO_3)_2$) to a solution of 50 µM L. The spectra were analysed and fit using HypSpec (HYPERQUAD suit of programs).[34]

ROS measurement: UV/Vis kinetic of ascorbate consumption experiments were recorded with a spectrophotometer Hewlett Packard Agilent 8453 or 8454 at a controlled temperature of 25 °C in 1 cm path length quartz cuvettes, with 800 rpm stirring.

The decrease of the ascorbate absorption band at λ_{max} = 265 nm (ε = 14 500 $M^{-1}.cm^{-1}$), systematically corrected at 800 nm, was plotted as a function of time. Unless specified, the samples were prepared *in situ* from stock solutions of L, L', Aβ, Zn(II) and Cu(II) at 1 mM diluted to 12 µM for L and L', Aβ and Zn(II) and 10 µM for Cu(II), in 100 mM HEPES buffer, pH 7.1. Some experiments were carried out with 2 equiv. of L (20 µM). Ascorbate was freshly prepared and diluted to 100 µM in the cuvette. The final volume in the cuvette was adjusted to 2 mL with milliQ water.

The ROS experiments were performed following three different procedures: starting from Cu(II), starting from Cu(I) and starting from a mixture of Cu(I) and Cu(II).

For the first experiment, L was added to a Cu(II) or Cu(II) + Aβ or Cu(II) + Aβ + Zn(II) mixture under aerobic conditions and then ascorbate was introduced in the cuvette.

For the second one, L was injected with Hamilton syringe to Cu(I) or Cu(I) + Aβ or Cu(I) + Aβ + Zn(II) in a sealed cuvette under anaerobic conditions and then was exposed to air. The Cu(I) was generated from the *in situ* reduction of Cu(II) with ascorbate. All the solution were previously degassed with argon 15 min before being introduced in the sealed UV-vis cuvette under argon.

For the last one (mixture of Cu(I) and Cu(II)), ascorbate was introduced first into the cuvette under aerobic conditions, then either Cu(II) or Cu(II) + Aβ or Cu(II) + Aβ + Zn(II) was added. When the absorbance was reaching about 1.17, L was added.

The ascorbate consumption rates were calculated during the last 25 minutes of the experiments by dividing the slope of the variation in ascorbate concentration by the extinction coefficient of ascorbate, ε = 14 500 $M^{-1}cm^{-1}$. Measurements were performed on at least three independent experiments, the average values are given in the text.

XANES. Cu(II) and Zn(II) K-edge XANES (X-ray absorption near edge structure) spectra were recorded at the BM30B (FAME) beamline at the European Synchrotron Radiation Facility (ESRF, Grenoble, France).[49] The storage ring was operated in 7/8+1 mode at 6GeV with a 200mA current. The beam

energy was selected using an Si(220) N_2 cryo-cooled double-crystal monochromator with an experimental resolution close to that theoretically predicted (namely ~ 0.5 eV FWHM at the Cu and Zn energy).[50] The beam spot on the sample was approximately 300 x 100 μm^2 (H x V, FWHM). Because of the low Cu(II) and Zn(II) concentrations, spectra were recorded in fluorescence mode with a 30-element solid state Ge detector (Canberra) in frozen liquid cells in a He cryostat. The temperature was kept at 20 K during data collection. The energy was calibrated with Cu and Zn metallic foils, such that the maximum of the first derivative was set at 8979 and 9659 eV. XANES Cu(II) data were collected from 8840 to 8960 eV using 5 eV step of 2 s, from 8960 to 9020 eV using 0.5 eV step of 3 s, and from 9020 to 9300 eV with a k-step of 0.05 $Å^{-1}$ and and 3 s per step. XANES Zn(II) data were collected from 9510 to 9630 eV using 5 eV step of 3 s, from 9630 to 9700 eV using 0.5 eV step of 3 s, and from 9700 to 10000 eV with a k-step of 0.05 $Å^{-1}$ and 3 s per step. For each sample, at least three scans recorded on different spots were averaged and spectra were background-corrected by a linear regression through the pre-edge region and a polynomial through the post-edge region and normalized to the edge jump. XANES samples were prepared from stock solution of peptide, ligands and metallic ions diluted down to approx. 1.0 mM in buffered solution. Samples were frozen in the sample holder after addition of 10% glycerol as a cryoprotectant and stored in liquid nitrogen until used. Cu(II) photoreduction was controlled by recording successive scans at the same spot. It was considered that during the first 20 minutes of recording the photoreduction is insignificant.

Electron Paramagnetic Resonance. Electron Paramagnetic Resonance (EPR) data were recorded using an Elexsys E 500 Bruker spectrometer, operating at a microwave frequency of approximately 9.5 GHz. Spectra were recorded using a microwave power of 2 mW across a sweep width of 150 mT (centered at 310 mT) with modulation amplitude of 0.5 mT. Experiments were carried out at 110 K using a liquid nitrogen cryostat.

EPR samples were prepared from a 0.1 M stock solution of ^{65}Cu (from $Cu(NO_3)_2$) diluted down to 200 µM in HEPES (50 mM, pH 7.1) with 1.2 equiv. of L. For the competition experiments, in an eppendorf tube, Cu (200 µM) was first mixed with Aβ (1.2 equiv.) (with or without 1.2 equiv. or 10 equiv. of Zn(II))

and then L (1.2 equiv.) was added to the solution. The mixture was stirred 5 min and transferred into an EPR tube. Samples were frozen in quartz tube, with addition of 10% glycerol as a cryoprotectant.

Conflicts of interest

There are no conflicts to declare.

Acknowledgements

RBMS thanks *CONACYT* for the PhD grant 439618. CH and CE thank the ERC aLzINK - Contract n° 638712 for financial support. CE thanks the PRESTIGE Programm for the grant n. PCOFUND-GA-2013-609102. RBMS thanks the FrenchBic for a grant allocated to his travel to Toulouse in CH's team to performed ROS experiments. CH and ACD warmly acknowledge the human support of FAME beamline at ESRF (project 30-02-1100) and collaborators who helped in the record of the data (Dr. F. Collin, Dr. S. Sayen and Prof. Guillon).

Supporting information available: structures of L and L'; L titrations with tetrakis(ACN)Cu(I) hexafluorophosphate $Zn(NO_3)_2$; X-band EPR spectra; competition experiments; kinetics of ascorbate consumption starting from Cu(II), Cu(I) and mixture; time evolution of UV-vis spectrum of Cu(I) + L; % of Cu(I) species; apparent affinity constants and single step reactions involved in mechanism.

Notes and references

1. Association, A. s., 2017 Alzheimer's disease facts and figures. *Alzheimer's & Dementia: The Journal of the Alzheimer's Association* **2017,** *13* (4), 325-373.
2. Hardy, J.; Higgins, G., Alzheimer's disease: the amyloid cascade hypothesis. *Science* **1992,** *256* (5054), 184-185.
3. Hureau, C., Coordination of redox active metal ions to the amyloid precursor protein and to amyloid-β peptides involved in Alzheimer disease. Part 1: An overview. *Coord. Chem. Rev.* **2012,** *256* (19), 2164-2174.
4. Atrián-Blasco, E.; Gonzalez, P.; Santoro, A.; Alies, B.; Faller, P.; Hureau, C., Cu and Zn coordination to amyloid peptides: From fascinating chemistry to debated pathological relevance. *Coord. Chem. Rev.* **2018,** *371*, 38-55.
5. Lovell, M. A.; Robertson, J. D.; Teesdale, W. J.; Campbell, J. L.; Markesbery, W. R., Copper, iron and zinc in Alzheimer's disease senile plaques. *J. Neurol. Sci.* **1998,** *158* (1), 47-52.

6. Miller, L. M.; Wang, Q.; Telivala, T. P.; Smith, R. J.; Lanzirotti, A.; Miklossy, J., Synchrotron-based infrared and X-ray imaging shows focalized accumulation of Cu and Zn co-localized with β-amyloid deposits in Alzheimer's disease. *J. Struct. Biol.* **2006,** *155* (1), 30-37.
7. Cheignon, C.; Tomas, M.; Bonnefont-Rousselot, D.; Faller, P.; Hureau, C.; Collin, F., Oxidative stress and the amyloid beta peptide in Alzheimer's disease. *Redox Biol.* **2018,** *14*, 450-464.
8. Cheignon, C.; Jones, M.; Atrián-Blasco, E.; Kieffer, I.; Faller, P.; Collin, F.; Hureau, C., Identification of key structural features of the elusive Cu–Aβ complex that generates ROS in Alzheimer's disease. *Chem. Sci.* **2017,** *8* (7), 5107-5118.
9. Atrián-Blasco, E.; del Barrio, M.; Faller, P.; Hureau, C., Ascorbate Oxidation by Cu(Amyloid-β) Complexes: Determination of the Intrinsic Rate as a Function of Alterations in the Peptide Sequence Revealing Key Residues for Reactive Oxygen Species Production. *Anal. Chem.* **2018,** *90* (9), 5909-5915.
10. Drew, S. C.; Barnham, K. J., The Heterogeneous Nature of Cu2+ Interactions with Alzheimer's Amyloid-β Peptide. *Acc. Chem. Res.* **2011,** *44* (11), 1146-1155.
11. Hureau, C.; Dorlet, P., Coordination of redox active metal ions to the amyloid precursor protein and to amyloid-β peptides involved in Alzheimer disease. Part 2: Dependence of Cu(II) binding sites with Aβ sequences. *Coord. Chem. Rev.* **2012,** *256* (19), 2175-2187.
12. Hureau, C., Metal Ions and Complexes in Alzheimer's Disease: From Fundamental to Therapeutic Perspectives. In *Encyclopedia of Inorganic and Bioinorganic Chemistry*, Scott, R. A., Ed. 2019; pp 1-14.
13. Alies, B.; Renaglia, E.; Rózga, M.; Bal, W.; Faller, P.; Hureau, C., Cu(II) Affinity for the Alzheimer's Peptide: Tyrosine Fluorescence Studies Revisited. *Anal. Chem.* **2013,** *85* (3), 1501-1508.
14. Conte-Daban, A.; Borghesani, V.; Sayen, S.; Guillon, E.; Journaux, Y.; Gontard, G.; Lisnard, L.; Hureau, C., Link between Affinity and Cu(II) Binding Sites to Amyloid-β Peptides Evaluated by a New Water-Soluble UV–Visible Ratiometric Dye with a Moderate Cu(II) Affinity. *Anal. Chem.* **2017,** *89* (3), 2155-2162.
15. De Gregorio, G.; Biasotto, F.; Hecel, A.; Luczkowski, M.; Kozlowski, H.; Valensin, D., Structural analysis of copper(I) interaction with amyloid β peptide. *J. Inorg. Biochem.* **2019,** *195*, 31-38.
16. Shearer, J.; Szalai, V. A., The Amyloid-β Peptide of Alzheimer's Disease Binds CuI in a Linear Bis-His Coordination Environment: Insight into a Possible Neuroprotective Mechanism for the Amyloid-β Peptide. *J. Am. Chem. Soc.* **2008,** *130* (52), 17826-17835.
17. Young, T. R.; Kirchner, A.; Wedd, A. G.; Xiao, Z., An integrated study of the affinities of the $A\beta_{16}$ peptide for Cu(I) and Cu(II): implications for the catalytic production of reactive oxygen species. *Metallomics* **2014,** *6* (3), 505-517.
18. Alies, B.; Badei, B.; Faller, P.; Hureau, C., Reevaluation of Copper(I) Affinity for Amyloid-β Peptides by Competition with Ferrozine—An Unusual Copper(I) Indicator. *Chem. Eur. J.* **2012,** *18* (4), 1161-1167.
19. Xiao, Z.; Gottschlich, L.; van der Meulen, R.; Udagedara, S. R.; Wedd, A. G., Evaluation of quantitative probes for weaker Cu(i) binding sites completes a set of four capable of detecting Cu(i) affinities from nanomolar to attomolar. *Metallomics* **2013,** *5* (5), 501-513.
20. Esmieu, C.; Ferrand, G.; Borghesani, V.; Hureau, C., N-truncated Aβ peptides impact on Cu and Cu(Aβ)-generated ROS: Cu(I) matters ! *Chem. Eur. J.* doi.org/10.1002/chem.202003949
21. Esmieu, C.; Guettas, D.; Conte-Daban, A.; Sabater, L.; Faller, P.; Hureau, C., Copper-Targeting Approaches in Alzheimer's Disease: How To Improve the Fallouts Obtained from in Vitro Studies. *Inorg. Chem.* **2019,** *58* (20), 13509-13527.
22. Savelieff, M. G.; Nam, G.; Kang, J.; Lee, H. J.; Lee, M.; Lim, M. H., Development of Multifunctional Molecules as Potential Therapeutic Candidates for Alzheimer's Disease, Parkinson's Disease, and Amyotrophic Lateral Sclerosis in the Last Decade. *Chem. Rev.* **2019,** *119* (2), 1221-1322.
23. Liu, Y.; Nguyen, M.; Robert, A.; Meunier, B., Metal Ions in Alzheimer's Disease: A Key Role or Not? *Acc. Chem. Res.* **2019,** *52* (7), 2026-2035.

24. Barnham, K. J.; Bush, A. I., Biological metals and metal-targeting compounds in major neurodegenerative diseases. *Chem. Soc. Rev.* **2014,** *43* (19), 6727-6749.
25. Savelieff, M. G.; Lee, S.; Liu, Y.; Lim, M. H., Untangling Amyloid-β, Tau, and Metals in Alzheimer's Disease. *ACS Chem. Biol.* **2013,** *8* (5), 856-865.
26. Pithadia, A. S.; Lim, M. H., Metal-associated amyloid-β species in Alzheimer's disease. *Curr. Opin. Chem. Biol.* **2012,** *16* (1), 67-73.
27. Conte-Daban, A.; Boff, B.; Candido, A.; Montes Aparicio, C.; Gateau, C.; Lebrun, C.; Cerchiaro, G.; Kieffer, I.; Sayen, S.; Guillon, E.; Delangle, P.; Hureau, C., A trishistidine pseudopeptide with ability to remove both Cu(I) and Cu(II) from the amyloid-beta peptide and to stop the associated ROS formation. *Chem. Eur. J.* **2017,** *23* (67), 17078-17088.
28. Conte-Daban, A.; Beyler, M.; Tripier, R.; Hureau, C., Kinetics Are Crucial When Targeting Copper Ions to Fight Alzheimer's Disease: An Illustration with Azamacrocyclic Ligands. *Chem. Eur. J.* **2018,** *24* (33), 8447-8452.
29. Vila-Real, H.; Coelho, H.; Rocha, J.; Fernandes, A.; Ventura, M. R.; Maycock, C. D.; Iranzo, O.; Simplício, A. L., Peptidomimetic β-Secretase Inhibitors Comprising a Sequence of Amyloid-β Peptide for Alzheimer's Disease. *J. Med. Chem.* **2015,** *58* (14), 5408-5418.
30. Leite, S. M. G.; Lima, L. M. P.; Gama, S.; Mendes, F.; Orio, M.; Bento, I.; Paulo, A.; Delgado, R.; Iranzo, O., Copper(II) Complexes of Phenanthroline and Histidine Containing Ligands: Synthesis, Characterization and Evaluation of their DNA Cleavage and Cytotoxic Activity. *Inorg. Chem.* **2016,** *55* (22), 11801-11814.
31. Rorabacher, D. B., Electron Transfer by Copper Centers. *Chem. Rev.* **2004,** *104* (2), 651-698.
32. Chassaing, S.; Collin, F.; Dorlet, P.; Gout, J.; Hureau, C.; Faller, P., Copper and Heme-Mediated Abeta Toxicity: Redox Chemistry, Abeta Oxidations and Anti-ROS Compounds. *Curr. Top. Med. Chem.* **2012,** *12* (22), 2573-2595.
33. Sokołowska, M.; Bal, W., Cu(II) complexation by "non-coordinating" N-2-hydroxyethylpiperazine-N'-2-ethanesulfonic acid (HEPES buffer). *J. Inorg. Biochem.* **2005,** *99* (8), 1653-1660.
34. Gans, P.; Sabatini, A.; Vacca, A., Investigation of equilibria in solution. Determination of equilibrium constants with the HYPERQUAD suite of programs. *Talanta* **1996,** *43* (10), 1739-1753.
35. James, B. R.; Williams, R. J. P., 383. The oxidation–reduction potentials of some copper complexes. *J. Chem. Soc.* **1961**, 2007-2019.
36. De Araujo, M. A.; Hodges, H. L., Electron-transfer reactions of copper complexes. 2. Kinetic investigation of the oxidation of bis(1,10-phenanthroline)copper(I) by tris(acetylacetonato)cobalt(III) and (ethylenediaminetetraacetato)cobalt(III) in aqueous and micellar sodium dodecyl sulfate solution. *Inorg. Chem.* **1982,** *21* (8), 3167-3172.
37. Hodges, H. L.; De Araujo, M. A., Kinetic investigation of the equilibrium between mono- and bis(1,10-phenanthroline)copper(I) in aqueous and sodium dodecyl sulfate solution. *Inorg. Chem.* **1982,** *21* (8), 3236-3239.
38. Noël, S.; Bustos Rodriguez, S.; Sayen, S.; Guillon, E.; Faller, P.; Hureau, C., Use of a new water-soluble Zn sensor to determine Zn affinity for the amyloid-β peptide and relevant mutants. *Metallomics* **2014,** *6* (7), 1220-1222.
39. Brandt, W. W.; Dwyer, F. P.; Gyarfas, E. D., Chelate Complexes of 1,10-Phenanthroline and Related Compounds. *Chem. Rev.* **1954,** *54* (6), 959-1017.
40. Goldstein, S.; Czapski, G., Mechanisms of the dismutation of superoxide catalyzed by the copper(II) phenanthroline complex and of the oxidation of the copper(I) phenanthroline complex by oxygen in aqueous solution. *J. Am. Chem. Soc.* **1983,** *105* (25), 7276-7280.
41. Conte-Daban, A.; Day, A.; Faller, P.; Hureau, C., How Zn can impede Cu detoxification by chelating agents in Alzheimer's disease: a proof-of-concept study. *Dalton Trans.* **2016,** *45* (39), 15671-15678.
42. Postnikova, G. B.; Shekhovtsova, E. A., Hemoglobin and myoglobin as reducing agents in biological systems. Redox reactions of globins with copper and iron salts and complexes. *Biochemistry (Moscow)* **2016,** *81* (13), 1735-1753.

43. Bernhard, S.; Takada, K.; Jenkins, D.; Abruña, H. D., Redox Induced Reversible Structural Transformations of Dimeric and Polymeric Phenanthroline-Based Copper Chelates. *Inorg. Chem.* **2002,** *41* (4), 765-772.
44. Miller, M. T.; Karpishin, T. B., Phenylethynyl Substituent Effects on the Photophysics and Electrochemistry of [Cu(dpp)2]+ (dpp = 2,9-Diphenyl-1,10-phenanthroline). *Inorg. Chem.* **1999,** *38* (23), 5246-5249.
45. Murali, M.; Palaniandavar, M., Mixed-ligand copper(II) complexes with positive redox potentials. *Transit. Met. Chem.* **1996,** *21* (2), 142-148.
46. Schwarzenbach, G.; Flaschka, H. A., *Complexometric titrations [by] G. Schwarzenbach & H. Flaschka*. 1969.
47. Smith, G. F.; Wilkins, D. H., New Colorimetric Reagent Specific for Cooper. *Anal. Chem.* **1953,** *25* (3), 510-511.
48. Teresa Albelda, M.; Alexandra Bernardo, M.; Garcia-España, E.; Luz Godino-Salido, M.; V. Luis, S.; João Melo, M.; Pina, F.; Soriano, C., Thermodynamics and fluorescence emission studies on potential molecular chemosensors for ATP recognition in aqueous solution *J. Chem. Soc., Perkin Trans.* **1999,** (11), 2545-2549.
49. Proux, O.; Biquard, X.; Lahera, E.; Menthonnex, J. J.; Prat, A.; Ulrich, O.; Soldo, Y.; Trvisson, P.; Kapoujyan, G.; Perroux, G.; Taunier, P.; Grand, D.; Jeantet, P.; Deleglise, M.; Roux, J. P.; Hazemann, J. L., FAME A New Beamline for XRay Absorption Investigations of VeryDiluted Systems of Environmental, Material and Biological Interests. *Phys. Scr.* **2005**, 970-973.
50. Proux, O.; Nassif, V.; Prat, A.; Ulrich, O.; Lahera, E.; Biquard, X.; Menthonnex, J.-J.; Hazemann, J.-L., Feedback system of a liquid-nitrogen-cooled double-crystal monochromator: design and performances. *J Synchrotron Radiat.* **2006,** *13* (1), 59-68.

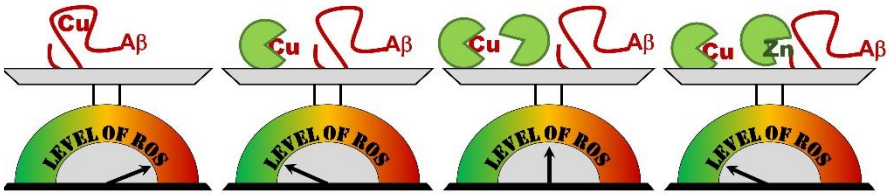

TOC. A phenanthroline peptide-like based ligand is able to remove Cu from Cu(Aβ) and redox silence it thus preventing Cu(Aβ)-induced ROS production. Excess of ligand lessens such a researched effect but Zn overrides it.